J Ind Microbiol Biotechnol (2014) 41:997–1006
DOI 10.1007/s10295-014-1440-5

SIMB
Society for Industrial Microbiology and Biotechnology

The effect of albumin fusion structure on the production and bioactivity of the somatostatin-28 fusion protein in *Pichia pastoris*

Yuedi Ding · Jun Fan · Wenxin Li · Ying Peng · Runlin Yang · Lili Deng · Qiang Fu

Received: 27 June 2013 / Accepted: 14 March 2014 / Published online: 22 April 2014

Abstract Somatostatin, a natural inhibitor of growth hormone (GH), and its analogs have been used in clinical settings for the treatment of acromegaly, gigantism, thyrotropinoma, and other carcinoid syndromes. However, natural somatostatin is limited for clinical usage because of its short half-life in vivo. Albumin fusion technology was used to construct long-acting fusion proteins and *Pichia pastoris* was used as an expression system. Three fusion proteins $(SS28)_2$-HSA, $(SS28)_3$-HSA, and HSA-$(SS28)_2$, were constructed with different fusion copies of somatostatin-28 and fusion orientations. The expression level of $(SS28)_3$-HSA was much lower than $(SS28)_2$-HSA and HSA-$(SS28)_2$ due to the additional fusion of the somatostatin-28 molecule. MALDI-TOF mass spectrometry revealed that severe degradation occurred in the fermentation process. Similar to the standard, somatostatin-14, all three fusion proteins were able to inhibit GH secretion in blood, with $(SS28)_2$-HSA being the most effective one. A pharmacokinetics study showed that $(SS28)_2$-HSA had a prolonged half-life of 2 h. These results showed that increasing the number of small protein copies fused to HSA may not be a suitable method for improving protein bioactivity.

Keywords Somatostatin · Albumin fusion · *Pichia pastoris* · Fusion orientation · Bioactivity · Expression level

Y. Ding (✉) · J. Fan · W. Li · Y. Peng · R. Yang · L. Deng · Q. Fu
Key Laboratory of Nuclear Medicine, Ministry of Health, Jiangsu Key Laboratory of Molecular Nuclear Medicine, Jiangsu Institute of Nuclear Medicine, Wuxi 214063, Jiangsu, China
e-mail: ding9912094@hotmail.com

Q. Fu
e-mail: fuqiang@jsinm.org

Introduction

Somatostatin was originally characterized as a hypothalamic peptide with a strong inhibitory effect on growth hormone (GH) secretion by the pituitary gland [2]. Somatostatin is a regulatory peptide that exerts a broad spectrum of actions in neurotransmission and hormone secretion from the anterior pituitary, pancreas, and gastrointestinal tract [8]. Moreover, somatostatin has been shown to inhibit secretion and growth in a number of neuroendocrine tumors [22]. Two biologically active forms of somatostatin, which consist of 14 (SS-14) or 28 (SS-28) amino acids, are present in the circulation and display tissue-specific expression. SS-28 is a naturally occurring, N-terminally extended form of tetradecapeptide SS-14 [20]. This peptide is the predominant molecular form of somatostatin in some tissues, and appears to be secreted. Furthermore, it has been shown to exhibit both higher or lower biological potencies compared to SS-14 in different target tissues and may possess its own receptors distinct from those of SS-14 [19].

Somatostatins mediate a diverse number of physiological actions by interacting with specific receptors in the plasma membrane [14, 25, 26]. Five somatostatin receptor subtypes have been cloned, namely sst1–5, though the sst2 somatostatin receptor exists in two splice variants sst2A and sst2B, which have a different carboxyl terminus [8, 14, 18]. The somatostatin receptors are expressed in both neuronal and non-neuronal tissues and tumors and have complex overlapping patterns of expression [24].

The unique pharmacological effects mediated by natural somatostatin are derived from its universal high-affinity binding to all somatostatin receptor subtypes sst1–sst5. However, natural somatostatin has a very short half-life of <3 min in vivo, limiting its therapeutic utility in humans [12]. As a result, synthetic derivatives have been designed

to produce more stable compounds. Among the many hundreds of somatostatin analogs, octreotide and lanreotide have been used to reduce or normalize excessive GH and insulin-like growth factor (IGF-1) levels associated with acromegaly [1, 27]. They are also widely employed in the therapy of somatotropin-secreting pituitary adenomas and neuroendocrine tumors of the gastroenteropancreatic system [17, 21]. However, these analogs bind preferentially to sst2 and sst5, with moderate affinity for sst3 and low affinities for sst1 and sst4 [11, 28]. The different binding affinity to the somatostatin receptors leads to limited pharmacological actions compared to natural somatostatin. Furthermore, unlike natural somatostatin, these analogs also showed a decreased response over long periods of administration, which was observed in the clinical usage of somatostatin analogs [23, 27]. These facts suggest that a new process to construct long-acting somatostatin analogs with the full pharmacological effects of natural somatostatin is highly desirable.

One approach aimed at improving the clinical effectiveness of small therapeutic proteins was to increase the molecular size of small proteins to above 50 kDa, e.g., expression via fusion proteins [15, 16]. Human serum albumin (HSA) fusion technology is a novel process based on the fact that fusing the heterogeneous proteins with a full-length HSA molecule extends their circulatory half-life in vivo while retaining their biological and therapeutic properties [3, 29]. This technology has been used to create long-acting forms of human interferon-α2b, human interleukin-2, human granulocyte-colony stimulating factor, human growth hormone, human insulin, and human glucagon-like peptide-1 [4, 5, 7, 15].

In this study, we designed three novel fusion proteins of human somatostatin-28 and HSA, designated $(SS28)_2$-HSA, $(SS28)_3$-HSA, and HSA-$(SS28)_2$, by genetically fusing the nucleotide sequence encoding two or three copies of human somatostatin-28 with the ORF of full-length HSA. These fusion proteins were constructed to compare the somatostatin bioactivity between different fusion orientations [$(SS28)_2$-HSA and HSA-$(SS28)_2$] as well as different fusion numbers [$(SS28)_2$-HSA and $(SS28)_3$-HSA]. The methylotrophic yeast *Pichia pastoris* is a highly successful system for the production of a variety of heterologous proteins. This system provides protein processing mechanisms, including signal peptide cleavage, protein folding, and posttranslational modifications, within the cell. Active proteins are secreted directly into the culture medium, thereby simplifying the purification process [6]. The *P. pastoris* expression system was used to produce the fusion proteins and the different expression levels between alternative fusion numbers and fusion orientations in *P. pastoris* were compared.

Materials and methods

Strains and materials

Escherichia coli JM109 (TaKaRa, Tokyo, Japan) and *P. pastoris* GS115 (Invitrogen Carlsbad, CA, USA) were used as the host strains for cloning and expressing fusion genes. The pMD19-T simple vector (TaKaRa) was used as a cloning vector, while the pPIC9K (Invitrogen) was used as an expression vector. Plasmid of pBluescript II KS (+)-*hsa* was kindly provided by Prof. Huazhong Li of Jiangnan University, China.

Construction of expression vectors

The *hsa* gene (GenBank accession No. NM_000477) was amplified from pBluescript II KS (+)-*hsa* and subcloned into the pMD19-T vector. In the forward primer 5′-gccggaattc**aaaaga**gatgcacacaagagtgaggttgctcatcgat-3′, the restriction sites *EcoRI* and *ClaI* are underlined and the sequence encoding lysine and arginine residues (site of Kex2 endoprotease) is in bold type. In the reverse primer 5′-cataaggcggccgc**ttatta**taagcctaaggcagcttg-3′, the restriction sites *SauI* and *NotI* are underlined and the stop codon is in bold type. The nucleotide sequence of the DNA inserted in the pMD19T-*hsa* vector was verified by DNA sequencing carried out by Sangon Biotech (Shanghai) Co. Ltd.

Two and three copies of somatostatin-28 genes [$(ss28)_2$ and $(ss28)_3$] were obtained by overlap PCR with nuclear sequences of 5′-tctgctaactcaaacccggctatggcaccccgagaacgcaaagctggctgcaagaatttcttctggaagactttcacatcctgttctgctaactcaaac-3′ and 5′-acaggatgtgaaagtcttccagaagaaattcttgcagccagctttgcgttctcggggtgccatagccgggtttgagttagcagaacaggatgtgaaagt-3′. Using the above extension product as a template, the upstream primer containing the *EcoRI* restriction site (underlined) and the sequence encoding lysine and arginine residues (bold) (5′-tgagaattc**aaaaga**tctgctaactcaaacccggctatggcaccccga-3′) and the downstream primer containing the *ClaI* restriction site (underlined) and the sequence encoding the N-terminal residues of HSA (bold) (5′-taa**atcgatgagcaacctcactcttgtgtgcatc**acaggatgtgaaag-3′) were applied to amplify the $(ss28)_2$ and $(ss28)_3$ genes for the construction of $(ss28)_2$-*hsa* and $(ss28)_3$-*hsa*. The expected 217-bp amplicon for $(ss28)_2$ and 300-bp amplicon for $(ss28)_3$ were subcloned into the pMD19T-*hsa* vector by the restriction enzyme ligation method and transformed into *E. coli* JM109. The correct integration of the inserts was checked by DNA sequencing.

Two primers, 5′-actg**ccttaggctta**tctgctaactcaaacccggct-3′and 5′-gatagcggccgc**ttaa**cacaggatgtgaaagtcttcca-3′, containing *SauI* and *NotI* cleavage sites respectively (underlined),

were used to amplify the $(ss28)_2$ gene for the construction of *hsa*-$(ss28)_2$. The sequence encoding the C-terminal residues of HSA (bold) was added in the forward primer and the stop codon (bold) was added in the reverse primer. The expected 198-bp amplicon was also subcloned into the pMD19T-*hsa* vector by restriction enzyme ligation method and verified by DNA sequencing.

Finally, the constructed fusion genes of $(ss28)_2$-*hsa*, $(ss28)_3$-*hsa*, and *hsa*-$(ss28)_2$ were digested with *EcoRI* and *NotI* and then inserted into the corresponding sites of the *P. pastoris* expression vector pPIC9K. The fusion genes were downstream to the alcohol oxidase I (AOX I) promoter and the α-factor signal sequence.

Transformation and expression of fusion proteins in *P. pastoris*

The recombinant plasmids pPIC9K-$(ss28)_2$-*hsa*, pPIC9K-$(ss28)_3$-*hsa*, and pPIC9K-*hsa*-$(ss28)_2$ were linearized with *SalI*, and transformed into *P. pastoris* GS115 cells by electroporation using a Micropulser apparatus (Bio-Rad, Hercules, CA, USA). His^+Mut^s recombinant clones were selected on MD plates (2 % dextrose, 4×10^{-5} % biotin, 1.34 % yeast nitrogen base, 1.5 % agar) after 3–4 days of incubation at 30 °C. Selected transformants were grown in 10 ml of BMGY medium (1 % yeast extract, 2 % polypeptone, 1.34 % yeast nitrogen base, 2 % glycerol, 4×10^{-5} % biotin, 0.1 M potassium phosphate buffer at pH 6.0) at 30 °C for 24 h under shaking at 200 rpm. The cells were harvested by centrifugation (5 min at 2,500 × *g*) and re-suspended in 3 ml of BMMY medium (BMGY with 2 % methanol instead of 2 % glycerol) to induce expression through the AOX promoter. The cultures were incubated at 30 °C for 72 h in a rotary shaker. Methanol was added every 24 h to a final concentration of 2 %. After 3 days of induction, the cultures were centrifuged (5 min at 10,000 × *g*) and the supernatants were quantified by Urine Microalbumin Kit (Shanghai Mind Bioengineering Co, Ltd, China) and checked by SDS-PAGE analysis followed by Coomassie blue straining.

High-cell-density fermentation at laboratory scale

The culture of the recombinant *P. pastoris* was seeded in two 500-ml shake flasks containing 100 ml of fermentation medium for 20 h under the condition of 30 °C and 220 rpm until $OD_{600} = 12$ was reached. The fed-batch fermentation was initiated in a 5-l bench-scale fermenter equipped with the standard DO/pH on-line measurement and control functions (BIOTECH-5BG, Baoxing Co., China), containing 2.5 l of BMMY medium (4 % glycerol). To control excessive foaming, 0.03 % (v/v) of antifoam 289 (Sigma, St. Louis, MO, USA) was added to the fermenter. The three phases in the fermentation, including glycerol batch phase, glycerol limited-feeding phase, and methanol induction phase, were conducted at 30 °C.

After 22-h cultivation without glycerol supplement, the initial batch phase ended with glycerol exhaustion indicated by a dissolved oxygen (DO) spike, and then followed by a 6-h transition phase with glycerol-limited feeding. During the second step, a mixed nutrition solution containing 500 ml of 5 × BMGY was supplied at the feeding rate of 125 ml/h. Due to the limited feeding, glycerol in broth was exhausted at 28 h, and the methanol induction phase began. Methanol was supplied at 120 ml/h for 20 s within 1 min after the DO was higher than 40 %. 5 × BMMY without methanol was supplemented at 13 ml/h during the whole induction phase to avoid degradation. After 70 h of cultivation, the fermenter was harvested and then the supernatant was collected by centrifugation (5 min at 10,000 × *g*, 4 °C) and filtered through a 0.45-μm membrane (Millipore, Bedford, MA, USA) before further analysis.

The pH was controlled by automatic addition of 2 M potassium hydroxide. DO was maintained within a suitable range by adjusting the agitation rate and using an oxygen-enriched system with the aid of a self-made air-oxygen mixer. During the fermentation, the temperature was maintained at 30 °C, while a stable pH value of 6.0 and a stable agitation speed of 800 rpm were also kept. The aeration rate was kept constant at 0.5 VVM.

Purification of fusion proteins

To purify the fusion protein in the supernatant, a one-step purification method using the Blue Sepharose affinity chromatography technique was performed. The supernatant was filtered through a 0.45-μm membrane and then ten-fold concentrated using an ultrafiltration device with a Biomax-10 membrane (Pellicon XL 50 Cassette and Labscale TFF System, Millipore) and loaded onto a Blue Sepharose 6 Fast Flow column (50 ml; flow rate 10 ml/min), which was equilibrated with a 20 mM phosphate buffer (pH 7.2, 0.15 M NaCl). After washing the column with one column volume (CV) of the same buffer, the fusion protein was eluted with 20 mM phosphate buffer (pH 7.2, 2 M NaCl). The eluate was dialyzed against water in MD34-14 dialysis tubing and freeze-dried (Labconco FreeZone, Kansas City, MO, USA).

Characterization of the fusion proteins

Western blot, mass spectrometry, and Edman N-terminal sequencing were used to characterize the fusion proteins. The purified proteins were separated with a 12 % SDS-PAGE gel and transferred onto a PVDF membrane (0.45 μm, Amersham Biosciences, Piscataway, NJ, USA) in a transfer buffer (24 mM Tris, 192 mM glycine, 20 %

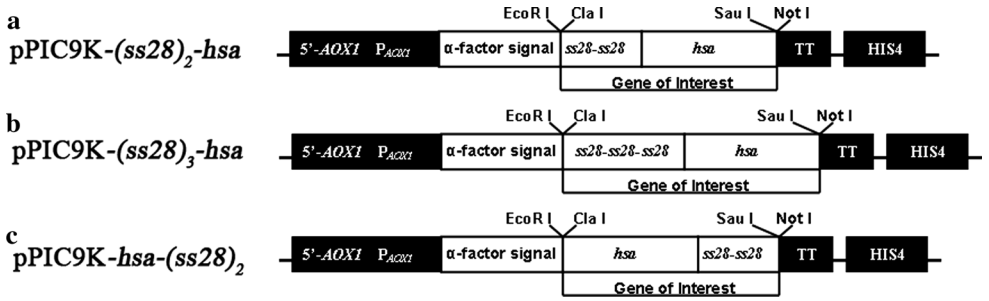

Fig. 1 Schematic of the fusion gene expression vectors, pPIC9K-$(ss28)_2$-*hsa* (**a**), pPIC9K-$(ss28)_3$-*hsa* (**b**), and pPIC9K-*hsa*-$(ss28)_2$ (**c**). The fusion genes encoding $(SS28)_2$-HSA, $(SS28)_3$-HSA, and HSA-$(SS28)_2$ were inserted into the pPIC9K vector along with the open reading frame of the α-factor signal under the control of the AOX1 promoter

methanol) at 100 V for 1 h. Then, the membrane was blocked with 5 % skimmed milk in TBST (0.01 M Tris–HCl, pH 7.5, 0.15 M NaCl, 0.05 % Tween-20) for 2 h at 37 °C and incubated with 1:500 diluted rabbit anti-somatostatin polyclonal (ab53165, Abcam, Cambridge, MA, USA) or rabbit anti-HSA polyclonal (ab83465, Abcam) at 4 °C overnight. The membrane was washed three times with TBST and incubated with 1:2,000 HRP-labeled goat anti-rabbit IgG (Santa Cruz Biotechnology, Santa Cruz, CA, USA) for 2 h at 37 °C. After sufficient washing, the ECL Western blotting luminol reagent (Santa Cruz) was used according to the manufacturer's protocol.

The fusion proteins were also analyzed by matrix-assisted laser desorption ionization-time of flight (MALDI-TOF) mass spectrometry with a Voyager DE-Pro mass spectrometer (Applied Biosystems, Foster City, CA). The lyophilized fusion proteins were mixed with a saturated solution of α-cyano-4-hydroxycinnamic acid containing 50 % (v/v) acetonitrile and 0.1 % (v/v) trifluoroacetic acid. The spectrum was obtained in direct mode and analyzed with the Voyager software version 5.0.

N-terminus sequencing was performed by Shanghai Applied Protein Technology Co. Ltd using a Procise Model 492 cLC protein sequencer (Applied Biosystems). After SDS-PAGE, the fusion proteins were electroblotted onto a PVDF membrane (Amersham Biosciences). The 70-kDa band on the PVDF membrane was cut out and used directly for repetitive Edman degradation followed by identification of the released amino acid derivates on HPLC.

Bioactivity analysis in vivo

Male BALB/c mice, approximately 6 weeks old on arrival, were purchased from Slac Laboratory Animal Co. (Shanghai, China) and housed in laminar airflow cabinets under pathogen-free conditions with a 12-h light/dark schedule and fed autoclaved standard chow and water ad libitum. Recombinant fusion proteins of $(SS28)_2$-HSA, $(SS28)_3$-HSA, and HSA-$(SS28)_2$ (10 mg/kg) were intravenously injected through the mouse tail. The control group was injected intravenously with somatostatin-14 standard (Sigma) at the dose of 0.15 mg/kg. Blood was collected from the ophthalmic venous plexus respectively at 0, 2, 6, and 24 h after administration and GH concentration in the plasma was measured using ELISA kit (R&D Systems, Minneapolis, MN, USA).

Pharmacokinetic analyses of $(SS28)_2$-HSA fusion protein

The pharmacokinetic behavior of fusion protein $(SS28)_2$-HSA following single-dose intravenous administration was evaluated in BALB/c mice. $(SS28)_2$-HSA, labeled with ^{125}I at its N-terminus, was prepared by Bolton-Hunter Reagents. Six BALB/c mice (male:female = 1:1) were injected intravenously with the ^{125}I labeled $(SS28)_2$-HSA at a dose of 5 mg/kg. Samples for plasma drug concentration were obtained at 5, 10, 15, 30, 60, and 90 min, 2, 4, 6, 12, and 24 h. The concentration of $(SS28)_2$-HSA in these samples was measured by radioactivity. The elimination half-life was calculated by Winnonlin v5.3 software (Pharsight Corporation, Mountain View, CA, USA).

Results

Vector construction and screening for high-level expression colonies

Fusion genes of $(ss28)_2$-*hsa*, $(ss28)_3$-*hsa*, and *hsa*-$(ss28)_2$, which were constructed by overlap PCR and restriction enzyme ligation method, were cloned into the *Eco*RI/*Not*I site of the pPIC9K vector along with the open reading frame of the α-factor signal under the control of the AOX1 promoter (Fig. 1). The plasmids with fusion genes were transformed into *P. pastoris* GS115 by electroporation, and positive transformants (His^+Mut^s) were selected on MD plates. For each fusion protein, nine colonies on the MD plate were selected and fermented according to *Pichia*

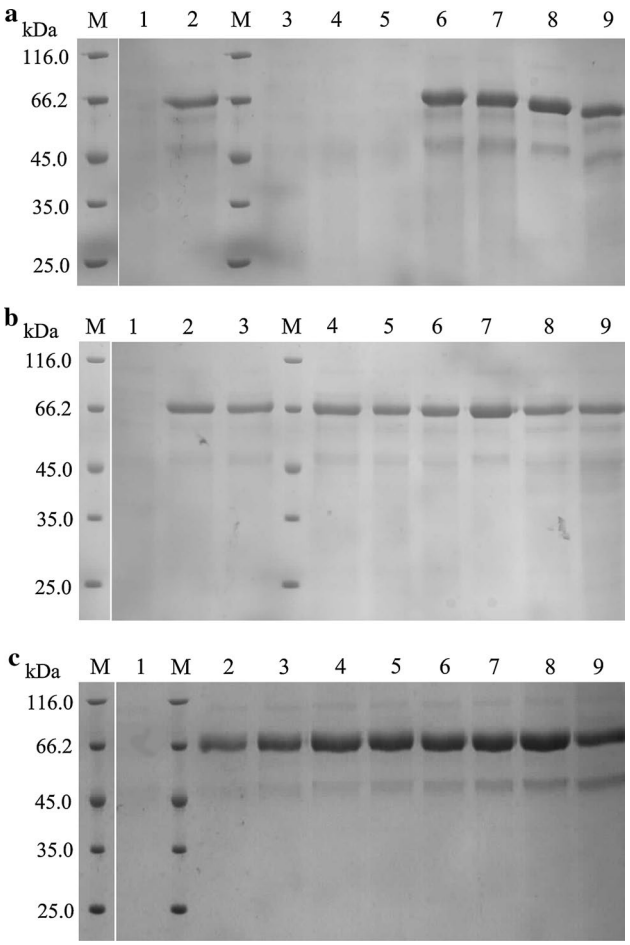

Fig. 2 SDS-PAGE analysis of fusion proteins expressed in *P. Pastoris* GS115. Twenty microliters of supernatant was applied to a 12 % SDS-PAGE and then stained with Coomassie brilliant blue. *M* sizes (kDa) of molecular weight markers. *Lanes 1–9* culture supernatants of GS115/pPIC9K/(*ss28*)$_2$-*hsa* (**a**), GS115/pPIC9K/(*ss28*)$_3$-*hsa* (**b**), and GS115/pPIC9K/*hsa*-(*ss28*)$_2$ (**c**) after 72 h of methanol induction

Expression Kit (Invitrogen). SDS-PAGE analysis showed that an obvious band around 70 kDa, which corresponds to the fusion proteins, was visualized in the original broth of recombinant strains, although some of strains did not express the protein of interest (Fig. 2). The strains with the highest expression level of (SS28)$_2$-HSA (230 mg/l), (SS28)$_3$-HSA (150 mg/l), and HSA-(SS28)$_2$ (250 mg/l) were chosen for next high-cell-density fermentation. For the obvious difference between the production of (SS28)$_2$-HSA and (SS28)$_3$-HSA, we believed that fusion numbers had a great effect on protein production in *P. pastoris* and the more copies of somatostatin-28 fused with HSA, the lower expression level would be obtained. Also, fusion orientations had little effect on protein production, as a modest difference was observed between (SS28)$_2$-HSA and HSA-(SS28)$_2$.

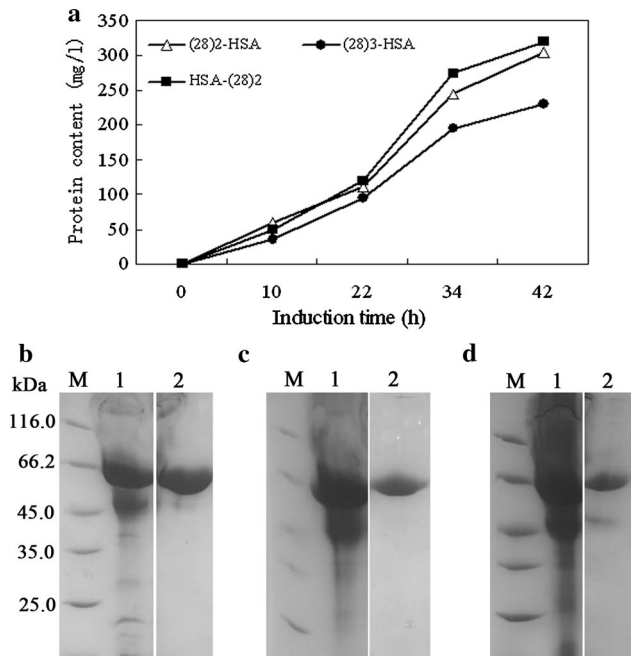

Fig. 3 **a** Time courses of (SS28)$_2$-HSA (*open triangle*), (SS28)$_3$-HSA (*solid circle*), and HSA-(SS28)$_2$ (*solid square*) production of recombinant *P. pastoris* GS115 in a 5-l fermenter during the induction phase. Purification of (SS28)$_2$-HSA (**b**), (SS28)$_3$-HSA (**c**), and HSA-(SS28)$_2$ (**d**) fusion proteins. Culture supernatants from the 5-l fermenter were tenfold concentrated by ultrafiltration (*lane 1*) and purified by Blue Sepharose affinity chromatography (*lane 2*)

High-cell-density fermentation and protein purification

In order to harvest large quantities of fusion protein, 5-l bench-scale of high-cell-density fermentation was conducted with the highest-yield recombinant strain isolated. After 28 h of fermentation with glycerol under batch and fed-batch conditions, which brought the cell concentration of OD_{600} above 180, the induction phase with pre-defined methanol feeding strategy was initiated. Figure 3a shows the time course of (SS28)$_2$-HSA, (SS28)$_3$-HSA, and HSA-(SS28)$_2$ production during the induction phase. Protein was harvested at 42 h of induction to avoid protein degradation. The cell growth of OD_{600} had been above 250 when the fermentation stopped and the protein concentration of (SS28)$_2$-HSA and HSA-(SS28)$_2$ had reached 305 and 320 mg/l, respectively, while (SS28)$_3$-HSA production had reached a lower level of 230 mg/l.

The culture supernatant was tenfold concentrated by ultrafiltration and purified by one-step Blue Sepharose affinity chromatographic procedure due to the high affinity between HSA and Blue Sepharose. The protein of interest (70 kDa) was adsorbed by Blue Sepharose and eluted by elution buffer. Besides, the extra band (100 kDa) had no affinity to Blue Sepharose and flowed through the column.

The degradation band (45 kDa), which had higher affinity with Blue Sepharose than the protein of interest, was also adsorbed by Blue Sepharose but could not be eluted by the elution buffer. As a result, the crude supernatant was purified by Blue Sepharose affinity column with the purity above 95 % (Fig. 3b–d).

Characterization of the fusion proteins

Western-blot analysis showed that all three of the fusion proteins could be recognized by both anti-somatostatin and anti-HSA rabbit polyclonal (Fig. 4a), indicating the presence of both somatostatin and HSA immunoreactivities in the fusion proteins.

The MALDI-TOF mass spectrometry was performed to analyze the recombinant fusion proteins, and results revealed that the molecular mass of $(SS28)_2$-HSA, $(SS28)_3$-HSA, and HSA-$(SS28)_2$ were 68,372.913, 68,793.470, and 67,843.204 Da, respectively (Fig. 4b–d). Compared with their calculated molecular mass (Table 1), a significant decrease was observed in these fusion proteins. $(SS28)_2$-HSA and HSA-$(SS28)_2$ both decreased more than 4 kDa in their calculated molecular mass, implying <1 somatostatin-28 molecule remained on the fusion proteins. Furthermore, $(SS28)_3$-HSA had an even deeper drop of 7 kDa, indicating more than two copies of somatostatin-28 was digested from the fusion protein. The significant decrease in molecular mass of fusion proteins demonstrated that severe degradation would occur in the fermentation process and showed the result that the more copies of somatostatin-28 fused to HSA, the more severe the degradation would be. Meanwhile, somatostatin-28 fused to the C-terminus of HSA suffered more severe degradation than when fused to the N-terminus. $(SS28)_2$-HSA decreased 4.4 kDa in molecular mass, less than the 4.9 kDa dropped by HSA-$(SS28)_2$.

Amino acid sequencing at the N-terminus of $(SS28)_2$-HSA was also performed by Edman degradation. Results showed that the N-terminal sequence (residues 1–5) of $(SS28)_2$-HSA was ERKAG, indicating the remaining protein fused with HSA was ERK-somatostatin-14, in agreement with its calculated molecular mass of 68,507.58 Da. Though the severe degradation leads only 17 amino acids remained to HSA, which between the molecules of intact somatostatin-14 and intact somatostatin-28, the 17 amino acids could still played the role of somatostatin.

Bioactivity analysis in vivo

Biological activity of recombinant $(SS28)_2$-HSA, $(SS28)_3$-HSA, and HSA-$(SS28)_2$ fusion proteins was tested by their inhibitory ability on GH secretion in vivo. Plasma GH concentration was measured in male BALB/c mice at 0, 2, 6, and 24 h after intravenous administration of fusion proteins. As shown in Fig. 5, similar to the standard somatostatin-14, all the fusion proteins could slightly inhibit GH secretion in blood after administration of 2 and 6 h, and were most effective when the drug was administrated over 24 h. Among these fusion proteins, $(SS28)_2$-HSA was most effective and mimicked the bioactivity of somatostatin-14.

Pharmacokinetic analyses of $(SS28)_2$-HSA

The pharmacokinetics of $(SS28)_2$-HSA were investigated in a BALB/c mouse model. The concentration of the $(SS28)_2$-HSA in plasma after a single intravenous dose of 5 mg/kg in mice was shown in Fig. 6. The elimination half-life of $(SS28)_2$-HSA was 2.07 h, which had been greatly prolonged by albumin fusion technique compared to the 3-min half-life of natural somatostatin.

Discussion

Somatostatin is a natural inhibitor of GH, glucagons, insulin, and chemical messengers like gastrin and vasoactive intestinal peptide. However, it has a very short half-life of <3 min, which limits its clinical usage. Octreotide, with a prolonged half-life of 2 h, is an octapeptide that mimics natural somatostatin pharmacologically, and has been approved by the US Food and Drug Administration (FDA) for the treatment of acromegaly, gigantism, thyrotropinoma, diarrhea, and flushing episodes associated with carcinoid syndrome, and diarrhea in patients with vasoactive intestinal peptide-secreting tumors (VIPomas). Albumin fusion is a novel strategy for improving the pharmacokinetics of small proteins or peptides. Production of long-lasting albumin fusion proteins can avoid complicated chemical modification or formulation processes. Pharmacokinetic properties and therapeutic efficacy of some albumin fusion proteins, such as interleukin-2 [10], glucagon-like peptide-1 [5], and interferon-α [15], have been tested to be efficiently improved.

We have characterized potent long-acting somatostatin analogs, $(SS28)_2$-HSA, $(SS28)_3$-HSA, and HSA-$(SS28)_2$, engineered using albumin fusion technology. We have expressed the fusion proteins in *P. pastoris*, which has been widely used to produce milligram-to-gram quantities of heterologous proteins, especially the production of recombinant human serum albumin (rHSA) [9, 13]. It was found that a significant production difference occurred between the three fusion proteins expressed in *P. pastoris*. $(SS28)_3$-HSA, three copies of somatostatin-28 fused with HSA, had only 60 % production compared to $(SS28)_2$-HSA and HSA-$(SS28)_2$, indicating that fusion of more copies of small protein with HSA to improve biological activity was

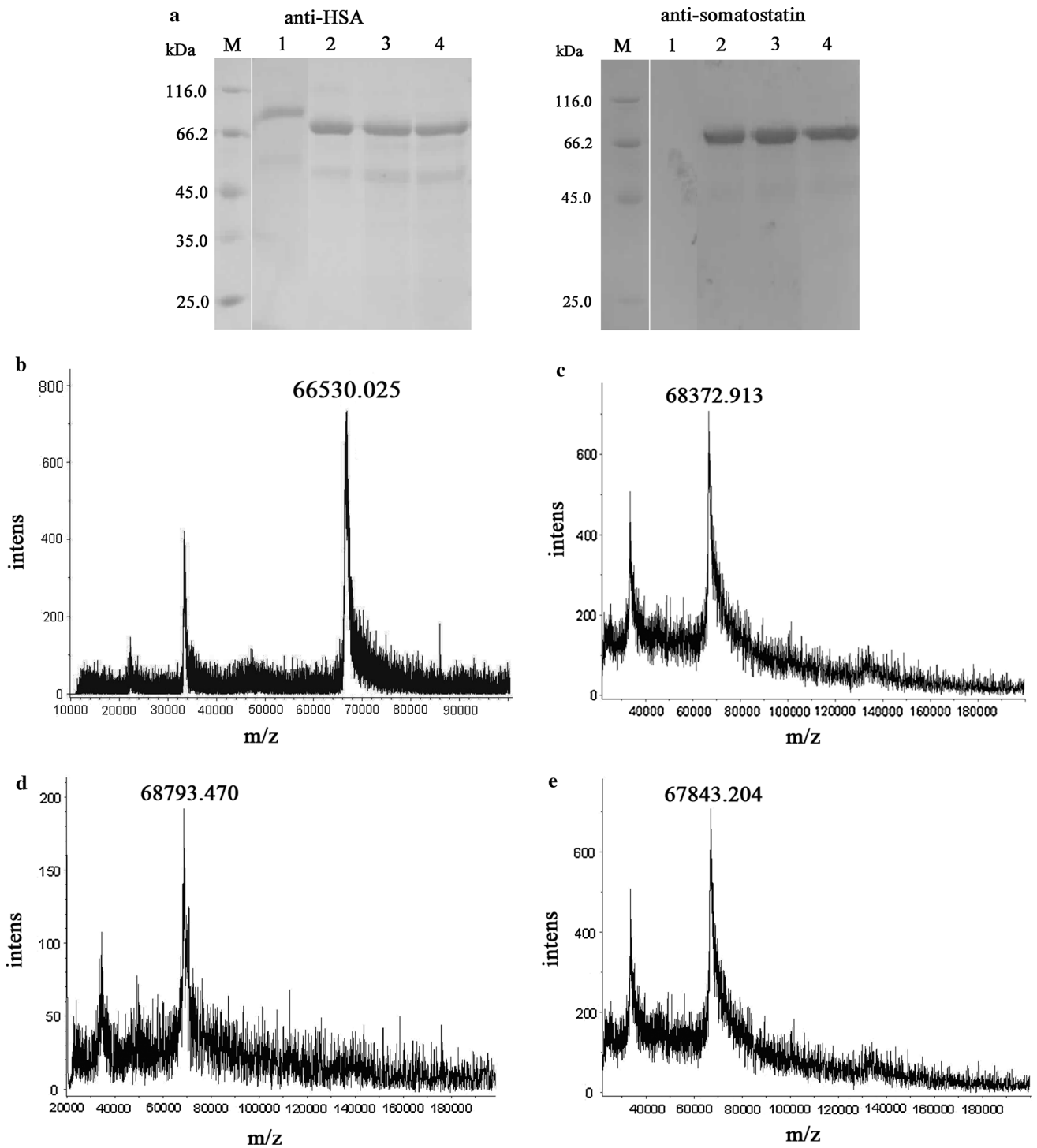

Fig. 4 Characterization of purified fusion proteins. **a** Western-blot analysis of HSA-IL-2 (*lane 1* as negative control), $(SS28)_2$-HSA (*lane 2*), $(SS28)_3$-HSA (*lane 3*), and HSA-$(SS28)_2$ (*lane 4*) immune reacted with anti-HSA polyclonal (*left*) and anti-somatostatin polyclonal (*right*). MALDI-TOF mass spectrometry of HSA (**b**), $(SS28)_2$-HSA (**c**), $(SS28)_3$-HSA (**d**), and HSA-$(SS28)_2$ (**e**)

not desirable at the production level. Results also showed that production of $(SS28)_2$-HSA and HSA-$(SS28)_2$ were almost at the same level, with only a slight increase occurring in HSA-$(SS28)_2$ compared to $(SS28)_2$-HSA, which may be the contribution of fusion orientations: the fusion of small proteins to the C-terminus of HSA was more potent in protein production than fusion to the N-terminus. For the production difference in *P. pastoris*, we conclude

Table 1 Comparison of calculated molecular mass and observed molecular mass in fusion proteins

Sample	Calculated molecular mass[a] (Da)	Observed molecular mass[b] (Da)	Decreased degree (Da)
$(SS28)_2$-HSA	72,737.37	68,372.913	4,364.46
$(SS28)_3$-HSA	75,869.96	68,793.470	7,076.49
HSA-$(SS28)_2$	72,737.37	67,843.204	4,894.17

[a] Calculated molecular mass showed the molecular mass calculated by compute pI/Mw (ExPASy) tool

[b] Observed molecular mass was detected by MALDI-TOF mass spectrometry

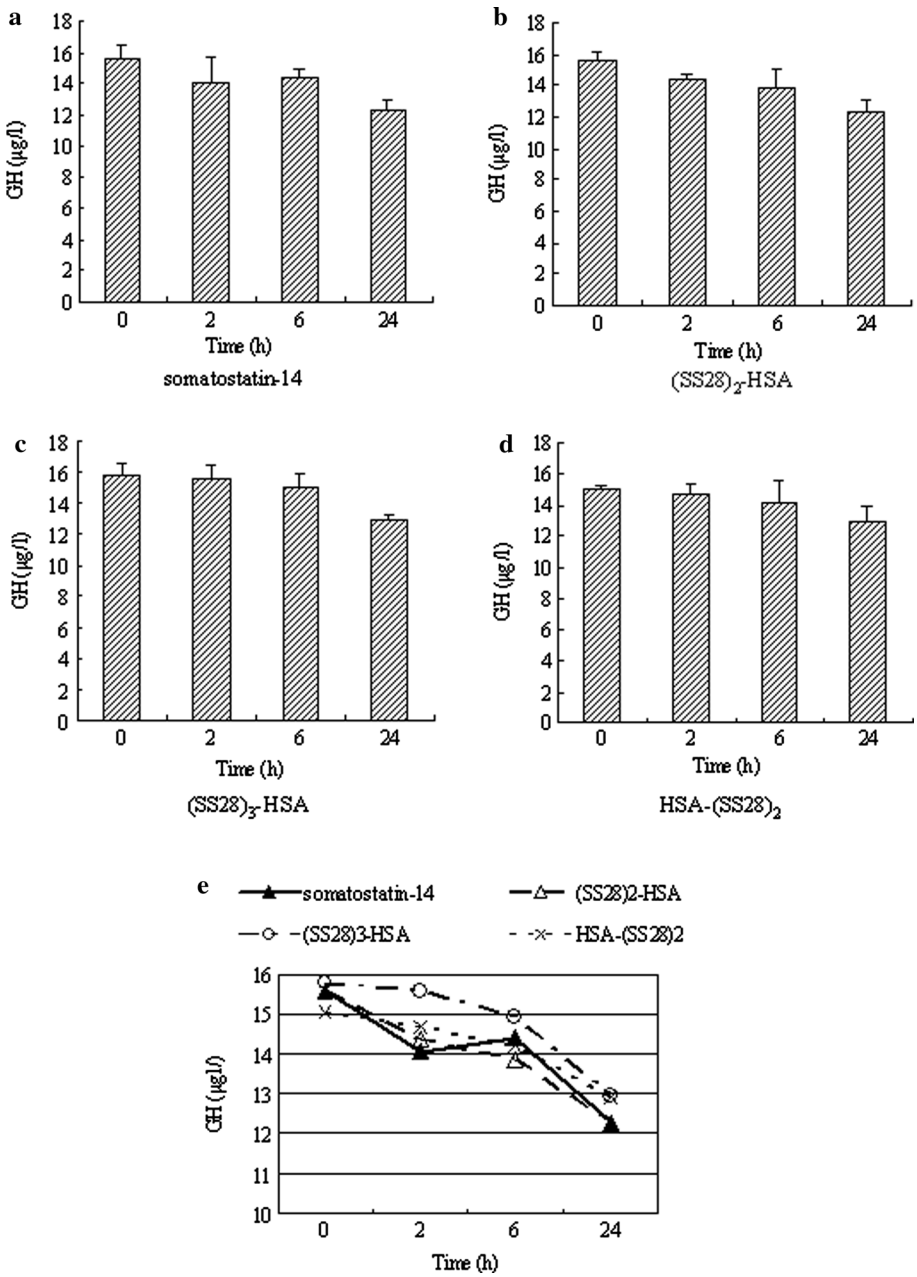

Fig. 5 Inhibitory effect of fusion proteins on GH secretion in mice plasma. Standard somatostatin-14 (**a**) and $(SS28)_2$-HSA (**b**), $(SS28)_3$-HSA (**c**), and HSA-$(SS28)_2$ (**d**) were intravenously injected into male BALB/c mice tail. At 0, 2, 6, and 24 h after administration, blood was collected from the ophthalmic venous plexus and GH concentration in the plasma was measured using an ELISA kit. **e** Bioactivity comparison of somatostatin-14 and three fusion proteins by the inhibitory ability on GH secretion. The data represent the means of three independent experiments (± standard error of the mean)

that the more copies of small protein there were that fused with HSA, the lower the expression level that would be obtained.

Fusion with albumin can decrease the protein's bioactivity because of increased spatial blockade [29, 30]. We postulated that increasing the fusion numbers of small protein

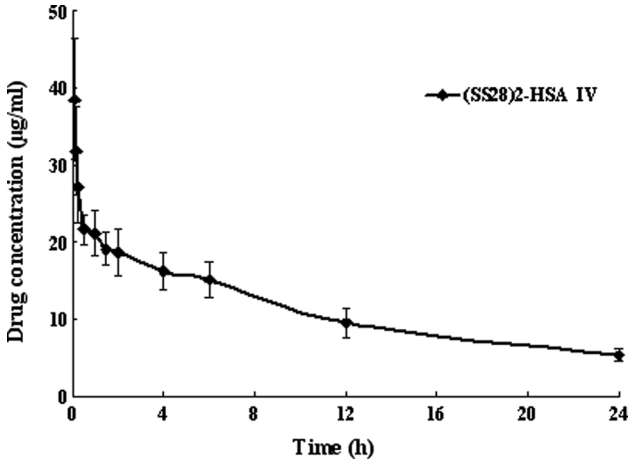

Fig. 6 Plasma concentration–time curve of $(SS28)_2$-HSA after a single-dose (5 mg/kg) intravenous administration in BALB/c mice. The *line* represents the mean (±SEM) data obtained from six mice sampled at each time point

would improve protein bioactivity, as more copies of small protein would increase the opportunity to bind with its receptor and the middle copy could act as a linker to make the new protein more flexible. So we designed two and three copies of somatostatin-28 fusion with HSA [$(SS28)_2$-HSA and $(SS28)_3$-HSA] to compare their biological activity. Simultaneously, the effect of fusion orientations [$(SS28)_2$-HSA and HSA-$(SS28)_2$] on protein bioactivity was also studied. However, it was disappointing to see, by MALDI-TOF mass spectrum analysis, that great degradation had occurred during the fermentation process. As more copies of somatostatin-28 were fused to HSA, more severe degradation also occurred. Observed molecular mass-by-mass spectrum showed that more than one copy of somatostatin-28 (3,150.60 Da) was digested from $(SS28)_2$-HSA and HSA-$(SS28)_2$ by endogenic protease in *P. pastoris* and more than two somatostatin-28 molecules were lost in $(SS28)_3$-HSA. Also, HSA-$(SS28)_2$ showed a lower molecular mass than $(SS28)_2$-HSA, which may indicate that fusing small proteins at the C-terminus of HSA suffers more severe degradation than fusion at the N-terminus, but the production level was slightly higher.

Bioactivity analysis revealed that $(SS28)_2$-HSA was the most effective one in GH inhibition, suggesting somatostatin-28 fusion at N-terminus of HSA was more effective than fusion at the C-terminus. Zhan et al. had previously studied the different bioactivity between shTNFRI-HSA and HSA-shTNFRI, and concluded that when HSA was fused at the N-terminus of shTNFRI, it could result in a larger degree of activity decline than when fused at the C-terminus. Fusion at the N-terminus might influence the posttranslational folding of the cysteine-rich domain (CRD) fragments and influence TNF-α binding, while fusion at the C-terminus seems to reduce the influence to some extent, and improve the stability as well as the recovery rate of the shTNFRs-HSA fusion protein [29]. In addition, more amino acids digested from HSA-$(SS28)_2$ than $(SS28)_2$-HSA could also be a reason for the decreased biological activity. The modest bioactivity of $(SS28)_3$-HSA also demonstrated that increasing the number of small protein copies fused to HSA was not a suitable method for improving the protein bioactivity.

In conclusion, we have developed three somatostatin-28 albumin fusion proteins with different fusion numbers [$(SS28)_2$-HSA and $(SS28)_3$-HSA] and fusion orientations [$(SS28)_2$-HSA and HSA-$(SS28)_2$] expressed in *P. pastoris*. $(SS28)_2$-HSA, with two copies of somatostatin-28 fused at the N-terminus of HSA, was the most effective one that mimicked the bioactivity of somatostatin-14 standard and had a prolonged half-life. So comparing the characterization of three fusion proteins, increasing the number of small protein copies fused to HSA may not be a suitable method for improving protein bioactivity.

Acknowledgments The authors thank Dr. Jian Jin and his colleagues for their technical assistance in fermentation and purification processes. The work was financially supported by the Natural Science Foundation of Jiangsu Province (BK2012104 and BK2011165) and the Public Service Platform for Science and Technology Infrastructure Construction Project of Jiangsu Province (BM2012066).

References

1. Ben-Shlomo A, Melmed S (2003) Clinical review 154: the role of pharmacotherapy in perioperative management of patients with acromegaly. J Clin Endocrinol Metab 88:963–968
2. Brazeau P, Vale W, Burgus R, Ling N, Butcher M, Rivier J, Guillemin R (1973) Hypothalamic polypeptide that inhibits the secretion of immunoreactive pituitary growth hormone. Science 179:77–79
3. Chang SH, Gong X, Yang ZY, Wang TY, Ma GC, Ma QJ, Wu J (2006) Expression in *Pichia pastoris* and properties of human serum albumin-interferon alpha2b chimera. Sheng Wu Gong Cheng Xue Bao 22:173–179
4. Dou WF, Lei JY, Zhang LF, Xu ZH, Chen Y, Jin J (2008) Expression, purification, and characterization of recombinant human serum albumin fusion protein with two human glucagon-like peptide-1 mutants in *Pichia pastoris*. Protein Expr Purif 61:45–49
5. Gao Z, Bai G, Chen J, Zhang Q, Pan P, Bai F, Geng P (2009) Development, characterization, and evaluation of a fusion protein of a novel glucagon-like peptide-1 (GLP-1) analog and human serum albumin in *Pichia pastoris*. Biosci Biotechnol Biochem 73:688–694
6. Gao Z, Li Z, Zhang Y, Huang H, Li M, Zhou L, Tang Y, Yao B, Zhang W (2012) High-level expression of the *Penicillium notatum* glucose oxidase gene in *Pichia pastoris* using codon optimization. Biotechnol Lett 34(3):507–514. doi:10.1007/s10529-011-0790-6
7. Halpern W, Riccobene TA, Agostini H, Baker K, Stolow D, Gu ML, Hirsch J, Mahoney A, Carrell J, Boyd E, Grzegorzewski KJ (2002) Albugranin, a recombinant human granulocyte colony stimulating factor (G-CSF) genetically fused to recombinant

human albumin induces prolonged myelopoietic effects in mice and monkeys. Pharm Res 19:1720–1729
8. Jacobs S, Schulz S (2008) Intracellular trafficking of somatostatin receptors. Mol Cell Endocrinol 286:58–62
9. Kobayashi K (2006) Summary of recombinant human serum albumin development. Biologicals 34:55–59
10. Lei J, Guan B, Li B, Duan Z, Chen Y, Li H, Jin J (2012) Expression, purification and characterization of recombinant human interleukin-2-serum albumin (rhIL-2-HSA) fusion protein in *Pichia pastoris*. Protein Expr Purif 84(1):154–160. doi:10.1016/j.pep.2012.05.003
11. Lesche S, Lehmann D, Nagel F, Schmid HA, Schulz S (2009) Differential effects of octreotide and pasireotide on somatostatin receptor internalization and trafficking in vitro. J Clin Endocrinol Metab 94:654–661
12. Lewis I, Bauer W, Albert R, Chandramouli N, Pless J, Weckbecker G, Bruns C (2003) A novel somatostatin mimic with broad somatotropin release inhibitory factor receptor binding and superior therapeutic potential. J Med Chem 46:2334–2344
13. Macauley-Patrick S, Fazenda ML, McNeil B, Harvey LM (2005) Heterologous protein production using the *Pichia pastoris* expression system. Yeast 22:249–270
14. Olias G, Viollet C, Kusserow H, Epelbaum J, Meyerhof W (2004) Regulation and function of somatostatin receptors. J Neurochem 89:1057–1091
15. Osborn BL, Olsen HS, Nardelli B, Murray JH, Zhou JX, Garcia A, Moody G, Zaritskaya LS, Sung C (2002) Pharmacokinetic and pharmacodynamic studies of a human serum albumin-interferon-alpha fusion protein in cynomolgus monkeys. J Pharmacol Exp Ther 303:540–548
16. Osborn BL, Sekut L, Corcoran M, Poortman C, Sturm B, Chen G, Mather D, Lin HL, Parry TJ (2002) Albutropin: a growth hormone-albumin fusion with improved pharmacokinetics and pharmacodynamics in rats and monkeys. Eur J Pharmacol 456:149–158
17. Pasquali D, Rossi V, Conzo G, Pannone G, Bufo P, De Bellis A, Renzullo A, Bellastella G, Colao A, Vallone G, Bellastella A, Sinisi AA (2008) Effects of somatostatin analog SOM230 on cell proliferation, apoptosis, and catecholamine levels in cultured pheochromocytoma cells. J Mol Endocrinol 40:263–271
18. Patel YC (1999) Somatostatin and its receptor family. Front Neuroendocrinol 20:157–198
19. Patel YC, Wheatley T (1983) In vivo and in vitro plasma disappearance and metabolism of somatostatin-28 and somatostatin-14 in the rat. Endocrinology 112:220–225
20. Pradayrol L, Jornvall H, Mutt V, Ribet A (1980) N-terminally extended somatostatin: the primary structure of somatostatin-28. FEBS Lett 109:55–58
21. Pyronnet S, Bousquet C, Najib S, Azar R, Laklai H, Susini C (2008) Antitumor effects of somatostatin. Mol Cell Endocrinol 286:230–237
22. Reubi JC (1997) Regulatory peptide receptors as molecular targets for cancer diagnosis and therapy. Q J Nucl Med 41:63–70
23. Schmid HA (2008) Pasireotide (SOM230): development, mechanism of action and potential applications. Mol Cell Endocrinol 286:69–74
24. Schulz S, Handel M, Schreff M, Schmidt H, Hollt V (2000) Localization of five somatostatin receptors in the rat central nervous system using subtype-specific antibodies. J Physiol Paris 94:259–264
25. Thermos K, He HT, Wang HL, Margolis N, Reisine T (1989) Biochemical properties of brain somatostatin receptors. Neuroscience 31:131–141
26. Thermos K, Reisine T (1988) Somatostatin receptor subtypes in the clonal anterior pituitary cell lines AtT-20 and GH3. Mol Pharmacol 33:370–377
27. van der Hoek J, van der Lelij AJ, Feelders RA, de Herder WW, Uitterlinden P, Poon KW, Boerlin V, Lewis I, Krahnke T, Hofland LJ, Lamberts SW (2005) The somatostatin analogue SOM230, compared with octreotide, induces differential effects in several metabolic pathways in acromegalic patients. Clin Endocrinol (Oxf) 63:176–184
28. Weckbecker G, Lewis I, Albert R, Schmid HA, Hoyer D, Bruns C (2003) Opportunities in somatostatin research: biological, chemical and therapeutic aspects. Nat Rev Drug Discov 2:999–1017
29. Zhan J, Chen Y, Yuan HY, Li H, Lu H (2012) Fusion of HSA influences TNF-alpha neutralizing activity of shTNFRs. Biotechnol Lett 34(3):417–423. doi:10.1007/s10529-011-0793-3
30. Zhao HL, Xue C, Wang Y, Li XY, Xiong XH, Yao XQ, Liu ZM (2007) Circumventing the heterogeneity and instability of human serum albumin-interferon-alpha2b fusion protein by altering its orientation. J Biotechnol 131:245–252